

# “Shadow effect” photodetector with linear output voltage vs light intensity

Cite as: J. Appl. Phys. 129, 203102 (2021); doi: 10.1063/5.0048655

Submitted: 25 February 2021 · Accepted: 8 May 2021 ·

Published Online: 24 May 2021



E. Hourdakis,<sup>a)</sup> A. Kaidatzis, and D. Niarchos

## AFFILIATIONS

NCSR Demokritos, Institute of Nanoscience and Nanotechnology, Patriarchou Grigoriou and Neapoleos 27, Aghia Paraskevi, 15341 Athens, Greece

<sup>a)</sup>Author to whom correspondence should be addressed: [m.hourdakis@inn.demokritos.gr](mailto:m.hourdakis@inn.demokritos.gr)

## ABSTRACT

A novel concept for a simple, cost effective, readily integrable with Si electronics and self-powered photodetector is presented. The device consists of a semitransparent Au film deposited on an n-type Si substrate with contacts on the Au layer. The operation of the device relies on the recently demonstrated “shadow effect.” The device is shown to consist of back-to-back Schottky diodes with a built-in parallel resistance caused by the Au layer. Shadowing half of the device area under illumination causes anisotropy in the diodes’ behavior creating a measurable open circuit voltage and a short circuit current. The presence of the built-in parallel resistance, along with a large series resistance, causes the open circuit voltage to have a linear term with respect to illumination power, in addition to the logarithmic term normally present in Schottky solar cells. We demonstrate that under certain combinations of series and parallel resistances the open circuit voltage of the device is linear with respect to illumination power for a range between 50 mW/cm<sup>2</sup> (0.5 sun) and 0.5 mW/cm<sup>2</sup> (0.005 sun). This allows the device to be used as a photodetector operated as a self-powered voltage source, instead of a current source which is the case with most photodetectors operated in the photovoltaic mode.

Published under an exclusive license by AIP Publishing. <https://doi.org/10.1063/5.0048655>

## INTRODUCTION

Photodetectors are an essential device in the field of optoelectronics. More specifically, the detection of the intensity of light has become very important in everyday applications such as smart building shading, lighting, and automatic car headlights. In this category of applications, cost is a very significant driving force. Moreover, with the advent of the Internet of Things (IoT), sensor systems inevitably move in the direction of self-powering.<sup>1–5</sup> This stems from the impractical nature of battery replacement in networks with large numbers of sensor nodes. Typical self-powered sensor systems are composed of an energy harvesting energy source and the sensor itself.<sup>2</sup> However, when a sensor does not require an external energy source for its operation, or when the sensor itself produces power, it can then be regarded as a self-powered sensor.<sup>3</sup> Of course, for a truly autonomous sensor system, there should be read out and communication electronics in addition to the sensor system. So, ideally, a photodetector designed for such everyday applications should be extremely cost effective, integrable with Si-based electronics and self-powered or, at the very least, not energy consuming. In addition, its output should be in a form that

is detectable and transmittable by the simplest electronic circuitry possible as a means to further reduce the cost and energy requirements of a system based on it.

The existing electronic photodetectors can be grouped into two main categories.<sup>6</sup> The first consists of the photoresistors.<sup>7–9</sup> In this case, ohmic contacts are created at the ends of a semiconductor piece and an external bias is applied. Incident light creates electron–hole pairs, which are separated by the external electric field increasing the current under constant bias conditions, or, effectively, changing the device resistance. These devices, despite their simplicity, require several processing steps for their fabrication, including photolithography for the definition of the ohmic contacts and the semiconductor shape, implantation, and/or high temperature annealing for the creation of the ohmic contacts and are energy consuming since they require an external bias and a current measurement.

The second category of photodetectors relies on the separation of light-induced electron–hole pairs by the photovoltaic effect. A built-in potential of a p-n, or a Schottky, diode separates the charges created by the absorbed light. Several variations of these

devices exist. For example, a p-n junction solar cell can be used as a photodetector even for small (indoor conditions) light intensities.<sup>10,11</sup> For such devices, the open-circuit voltage of the sensor ( $V_{oc}$ ) drops logarithmically as the power of the incident light decreases, while the short-circuit current ( $I_{sc}$ ) linearly.<sup>12–15</sup> A measurement of the current is therefore more appropriate in these devices. In order to facilitate the charge collection efficiency and improve some performance parameters,<sup>16,17</sup> an external reverse bias is often applied.<sup>6</sup> In such a case, the obvious advantage of these devices as operating without externally supplied power disappears. p-n junction based devices require a large number of processing steps, which include implantation steps and large temperature annealings both for the junction itself but also, in some cases, for the backside ohmic contacts. So, despite their excellent performance, these devices are not cost-optimized, or optimized in terms of their environmental footprint.

Schottky barrier based devices are similar to the p-n junction ones, without the need for the implantation steps, which makes them more attractive in terms of processing and cost.<sup>18–20</sup> Also, there are variations of these devices that are more flexible than their p-n junction counterparts. For example, Metal–Semiconductor–Metal (MSM) photodetectors are devices that can be integrated solely on the top side of a wafer making them suitable for back-end processing.<sup>21,22</sup> In this case, electrodes (usually interdigitated) are integrated on top of a semiconductor creating back-to-back Schottky diodes. The application of an external bias forces one diode to be reverse biased (increasing its depletion width), while the other to be forward biased (decreasing its depletion width). As before, the current induced by incident light (this time in the region of the semiconductor in between the electrodes) varies linearly with its power. These devices are simple to fabricate, but suffer from their power consumption and the need to measure current.

Recently, an interesting idea named the “shadow effect” was presented describing how a Schottky junction can be used to detect shadows and use shadows to harvest power from light.<sup>23–26</sup> In short, it has been demonstrated that by shadowing a part of Schottky diode under illumination an electrical imbalance is produced between the “shadowed” and the “illuminated” parts of the device leading to the creation of significant  $V_{oc}$  and  $I_{sc}$  with a very simple device structure. This idea has been used for the harvesting of energy from light in a variety of applications.<sup>23,25,26</sup> It has also been used as a method of detecting the position of a light pulse or a shadow.<sup>23,24</sup> The advantages of the shadow effect are its simplicity, in terms of device structures possible, and its integrability with back-end processes.

We have used this idea, “the shadow effect,” to create a novel photodetector that is extremely cost effective and requires no external energy source. The presented sensor is markedly different from the previous devices based on the “shadow effect,” even though its structure is very similar. Our device is a true photodetector in that it measures the intensity of light and not the position of a light pulse or a shadow. More specifically, the concept presented allows for a linear output voltage of the sensor as a function of light intensity, something that has not been presented before. This novelty offers the significant advantage of reduced complexity of readout electronics and energy consumption. We believe that this fact

makes this device appropriate for low-cost applications where performance is not the driving factor. In contrast to the previous work, the energy harvested by our device is not aimed at powering other sensors or actuators but it is rather used for the “self-powering” of the sensor itself. A simple electrical equivalent model is provided to explain the operational principle of the presented device, something not found in the previous “shadow effect” publications. We believe that the presented photodetector is a significant advancement toward the creation of affordable, everyday applications, based on the detection of light intensity.

## RESULTS AND DISCUSSION

### Photodetector structure and measurement configuration

The device structure was similar to the ones presented in Ref. 23. A thin Au layer was deposited by magnetron sputtering on top of an n-type Si sample (1–2  $\Omega$  cm) after removal of the native oxide by an HF dip. Au was chosen as it forms a well-studied Schottky barrier with n-type Si.<sup>27,28</sup> Magnetron sputtering physical vapor deposition (PVD) was chosen because it is a coating method compatible with industrial microelectronics processes (i.e., high volume production of low-cost devices). A thickness of 15 nm was chosen for the Au film as a direct comparison to the results of Ref. 23 and to allow enough transparency for light to be absorbed by the underlying Si substrate. The device size was 2 cm by 1 cm, as a compromise between comparison to Ref. 23 and a more practical size for applications. Transmittance (%) as a function of wavelength for the deposited Au film is presented in Fig. 1(a). The peak present around 550 nm is characteristic of the Au film.<sup>29</sup> The current density as a function of applied voltage for the Au/Si Schottky junction is presented in Fig. 1(b), along with a schematic of the measurement polarity. For these measurements, smaller devices (0.1 mm by 1 mm) were used, so the current was noisy near its lowest point (the noise in our system was at the  $10^{-9}$  A level). Nevertheless, our devices clearly satisfy both criteria, namely, transparency and the creation of a Schottky diode.

In order to characterize the devices, mechanical contacts (probes) were placed roughly in the middle of each half of the device. So the two contacts are connected by back-to-back Schottky diodes with a series resistance of the Si substrate ( $R_{Si}$ ) in between and by a parallel resistance ( $R_p$ ) of the Au layer. A schematic representation of the device is presented in Fig. 2(a), along with an energy diagram. A top-down photograph of the device is also provided with the corresponding contacts and leads. In this picture, the red lead corresponds to the higher voltage while the black corresponds to the ground of the measurement system. We note that the device is extremely simple to fabricate and requires practically no processing.

The device behavior under illumination was studied under a solar simulator. In order to achieve an asymmetry by the “shadow effect,” a non-transparent metallic piece was used to mask half of the device as shown in Fig. 2(b). By doing so, under illumination, electron–hole pairs are created in the depletion region only on the illuminated part of the device causing a current to flow through it, as is schematically shown in the energy diagram of Fig. 2(b). Mechanical masking was chosen for demonstration purposes only.

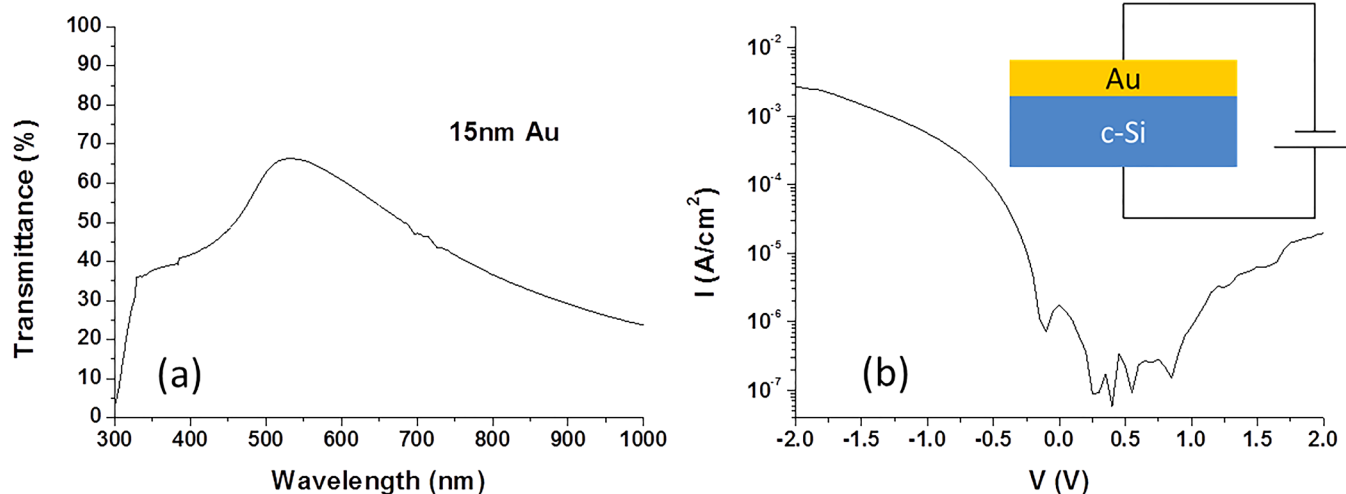


**FIG. 1.** (a) Transmittance as a function of the wavelength of light for the deposited 15 nm thick Au film. (b) Current density as a function of applied voltage for the Au/Si Schottky diode. A schematic representation of the measurement setup appears in the inset.

As was also shown in Ref. 23, the conditions used (50% shading and contacts in the middle of each half) provide the maximum output characteristics.

We note that the structure of these devices is similar to lateral photovoltaic effect devices.<sup>30–32</sup> These have mainly been used for the creation of Position Sensitive Photodiodes (PSDs).<sup>30</sup> The difference between PSDs and our devices is that in our case, this simplified structure is used to create a broad wavelength photodetector and not a light position sensor. In addition, the “shadow effect” is used in our case, rather than a local illumination of the device by a spatially limited light source. The non-trivial full theoretical analysis of non-uniformly illuminated junctions has been described within these publications.<sup>30–32</sup> In the following, we present a simplified approach of addressing our device under the illumination conditions described herein, through an equivalent electrical circuit model, therefore bypassing the significant efforts needed to solve the related differential equations.

### Principle of operation

To better understand the operation of the described device under illumination, an equivalent circuit is presented in Fig. 3. The circuit of Fig. 3 is not a direct representation of the schematics in Fig. 2, but it allows explaining the operating principle in the simplest way. Going from the illuminated contact to the dark one, a series resistance for the Au layer has to be taken into consideration due to its small thickness and the large area of the Schottky contacts (1 cm<sup>2</sup>). The Schottky diode in the dark ( $S_D$  in Fig. 2) also acts as a series resistance in this case. Its value may change slightly according to the current flowing through the device, but since these currents are small and this diode is always forward biased, we have bundled it along with the Au contact series resistance and the Si resistance ( $R_{Si}$ ) into one series resistance ( $R_S$ ). The dark diode is always forward biased by the current originating at the diode under

illumination, as can be seen by the energy diagram of Fig. 2(b). Note that this is an “internal” series resistance of the device. An “external” one ( $R_S$ ) also exists due to the contact resistance of the probes, the resistance of the wires, etc. For the presented device,  $R_S$  will always be much smaller than  $R_S$  because of the relatively large resistance of the  $S_D$ , the series resistance of the thin Au layer, and the resistance of the Si substrate. The “built in” parallel resistance ( $R_P$ ) describes the resistance of the continuous Au film in between the two contacts. The effect of the illumination is usually represented as a current source  $I_L$  across the illuminated junction  $S_L$ . The open circuit voltage condition is represented by the measurement of  $V_m$  in Fig. 3(a). This is not the same as the  $V_{oc}$  of  $S_L$ , in this case, as the presence of  $R_P$  will cause the flow of a current through the device internally. The short circuit current condition is represented by the measurement of  $I_m$  in Fig. 3(b), again distinguishing it from the  $I_{sc}$  of the Schottky diode  $S_L$ . We finally note that we have neglected the Schottky diode shunt resistance in our model due to its normally large value and the fact that  $R_P$  is rather small in our case.

The following analysis of the equivalent circuits of Fig. 3 follows from the discussion of the effects of the series and parallel resistances on an illuminated junction described in Ref. 33. The main difference is the fact that in our case, a Schottky diode rather than a p-n diode is present.

In order to understand the behavior of the presented device, we note that in Fig. 3(a) the photocurrent  $I_L$  flows through the illuminated junction  $S_L$  and the resistance  $R_P$ , while in the case of Fig. 3(b)  $I_L$  is first divided between  $S_L$  and  $R_S$  and then the current through  $R_S$  is divided again between  $R_P$  and  $R_S$ .

The current through  $S_L$  can be written in the form<sup>6</sup>

$$I_{S_L} = I_0 \left( \frac{e^{V_{S_L}}}{e^{nk_B T}} - 1 \right), \quad (1)$$

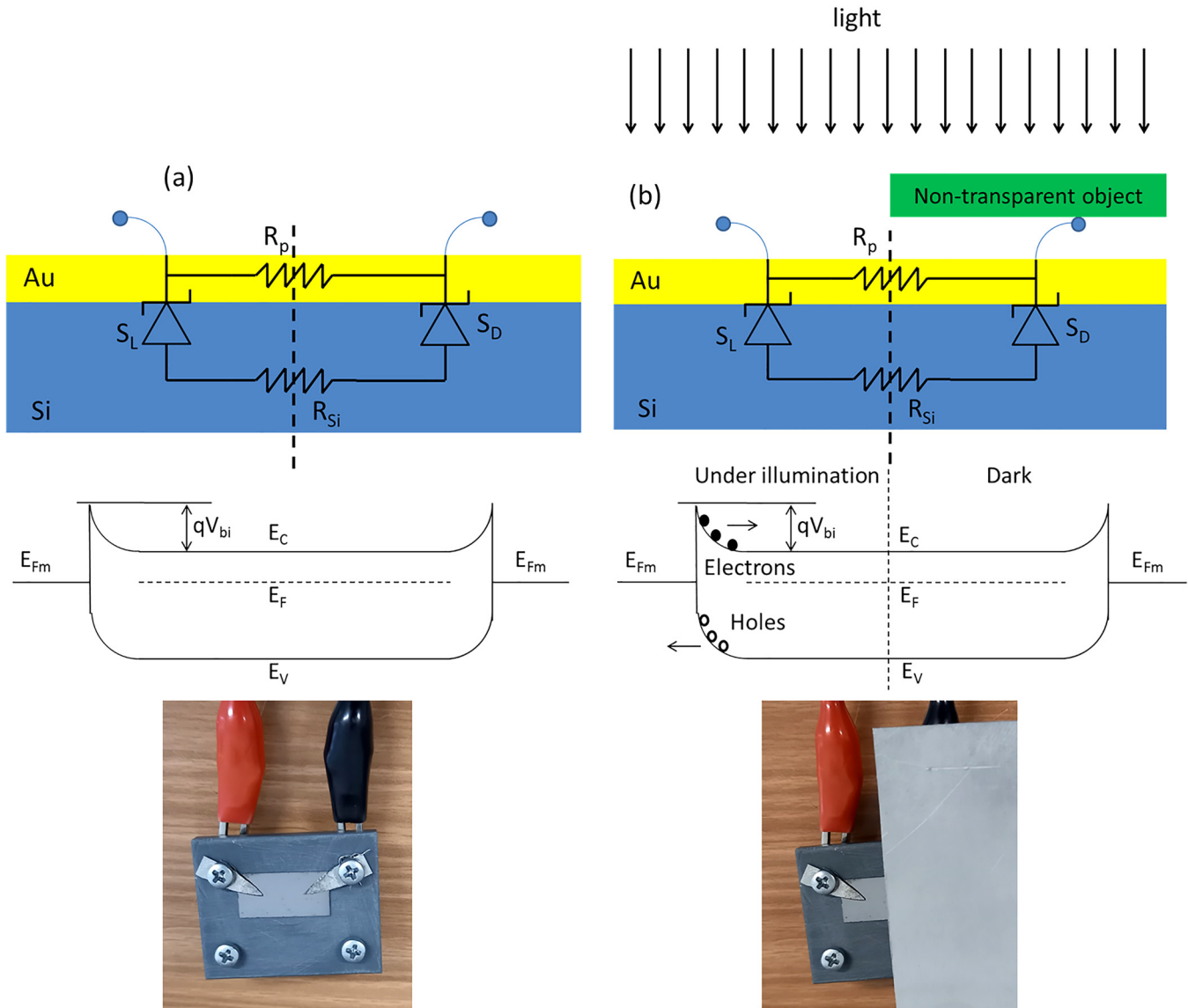


FIG. 2. Schematic representation of the device along with an energy diagram and a photograph in (a) the dark and (b) under illumination.

where  $I_0$  is usually referred to as the leakage current of the diode and depends on the barrier height, the area of the junction, the temperature, and the materials used (as well as their doping concentration);  $n$  is the ideality factor;  $k_B$  is the Boltzmann constant;  $T$  is the temperature;  $e$  is the electron charge; and  $V_{SL}$  is the voltage across the junction  $S_L$ . For the open circuit condition of the  $V_m$  measurement, it can be seen from the equivalent circuit of Fig. 3(a) that

$$V_m = \frac{R_p}{R_p + R_S} V_{SL}, \quad (2)$$

where  $V_{SL}$  is the voltage across junction  $S_L$  and

$$I_L = I_0 \left( \frac{e^{V_m (R_p + R_S)}}{R_p} - 1 \right) + \frac{V_m}{R_p}, \quad (3)$$

$$I_L = KE, \quad (4)$$

where  $K$  depends on the area of the illuminated side and the transparency of the Au film and  $E$  is the illumination power per  $\text{cm}^2$ . The combination of Eqs. (3) and (4) provides a direct relation between the intensity of the light (or the illumination power  $E$ ) and

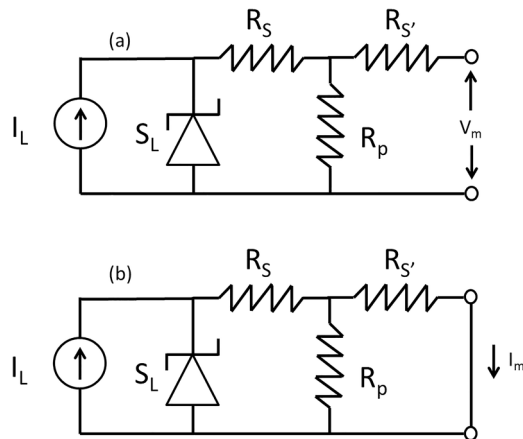


**FIG. 3.** Simplified equivalent circuit of the proposed photodetector under illumination for (a) the open voltage  $V_m$  and (b) the short circuit current  $I_m$ . In both diagrams,  $I_L$  is the photocurrent generated by the Schottky diode  $S_L$  under illumination,  $R_S$  is the “internal” series resistance including the resistance of the dark Schottky diode and the Si resistance,  $R_p$  is the “internal” parallel resistance of the Au film, and  $R_{S'}$  is the “external” series resistance of the contacts and wires.

the measured open-circuit voltage of the device  $V_m$ . In contrast to Schottky solar cells and MSM photodetectors, the presence of the “built-in” parallel resistance adds a linear part in Eq. (3). This is the equivalent of measuring the voltage across an external load of a solar cell but integrated into the device and fabricated with minimal processing.

From Fig. 3(b), it can be calculated that

$$I_L = I_0 \left( e^{\frac{eI_m}{nk_B T} \left( \frac{(R_p + R_{S'})R_S}{R_p} + R_{S'} \right)} - 1 \right) + I_m \frac{(R_p + R_{S'})}{R_p}. \quad (5)$$

For the condition that  $R_{S'} \ll R_p$ ,  $R_S$  Eq. (5) becomes

$$I_L = I_0 \left( e^{\frac{eI_m}{nk_B T} (R_S)} - 1 \right) + I_m. \quad (6)$$

Under certain conditions of  $R_S$  and  $R_p$  for a given  $I_L$  and  $I_0$ , the linear term in Eq. (3) and the exponential term in Eq. (6) become dominant and this is the basis of operation of the photodetector presented in this work.

For a given  $R_p$  (or a given thickness of the Au layer),  $V_m$  is maximum when  $V_{SL}$  is maximum and  $R_S$  is minimum. This can be achieved when half of the device is illuminated and half is in the dark. Illuminating a larger portion of the device will increase  $I_L$ , which, in turn, will increase  $V_{SL}$ , but it will also increase the series resistance of  $S_D$ . On the other hand, illuminating a smaller portion of the device will decrease the series resistance but will also decrease  $I_L$  and therefore  $V_{SL}$ . Also, the position of the probes affects  $V_m$  through the series resistance, this time the portion of it is affected by the resistance of the Au film. The minimum possible

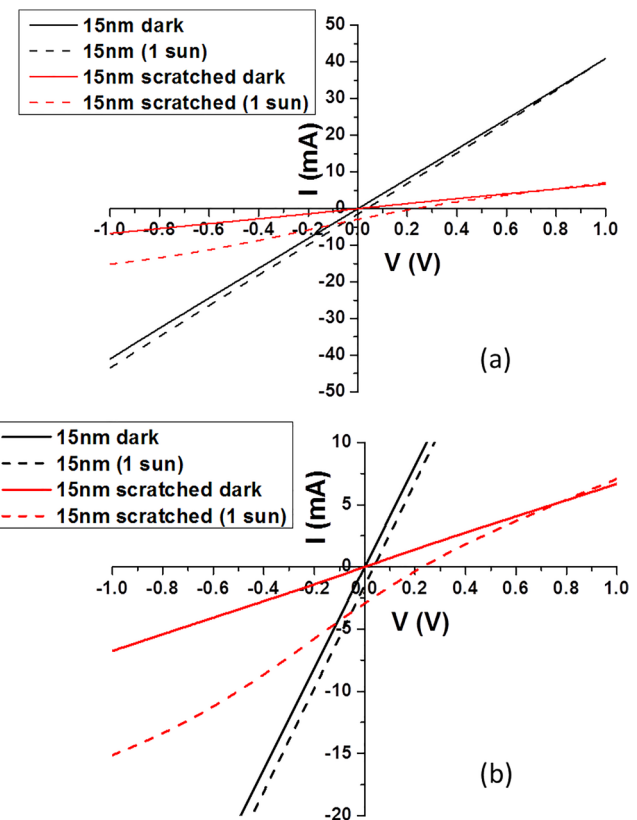


**FIG. 4.** I–V characteristics of the devices with 15 nm (black lines) and 15 nm scratched (red lines) Au films in the dark (solid lines) and under illumination (dashed lines). Part (b) is a magnification of part (a).

value is when the probes are positioned in the center of the “illuminated” and “dark” sides of the devices.

### Device characterization

In order to characterize the device described in Fig. 2, current–voltage characteristics are measured. In the following, the open circuit voltage ( $V_m$ ) presented in Fig. 3(a) is described by the x-axis intercept of the data, while the short circuit current ( $I_m$ ) presented in Fig. 3(b) is described by the y-axis intercept, as is standard in photovoltaic devices. The measured current through the devices with 15 nm Au in the dark and under 1 sun (100 mW/cm<sup>2</sup>) illumination is presented in Fig. 4 as black solid and dashed lines, respectively. Figure 4(b) is just a magnification of Fig. 4(a). It can be easily seen that the I–V curves appear linear, a clear indication that the behavior of the device is dominated by the parallel resistance  $R_p$ . Even so, a clear and measurable  $V_m$  and  $I_m$  exist, their values being 35 mV and 1.48 mA, respectively. The value of  $V_m$  is an order of magnitude less than the expected value for Au/Si Schottky contacts.<sup>27,28</sup> It is, however, expected since, from Eq. (2), as  $R_p$  goes to zero, so does  $V_m$ .



In order to increase  $V_m$ ,  $R_p$  was increased by scratching the Au film using tweezers. A scratch across the sample at the very center of it was created with a width of 2 mm separating the dark and illuminated parts of the samples. Scratching the Au layer with the tweezers ensures that not all of the Au is removed from the scratched area and that  $R_p$  is increased without the need for additional processing. The effect of the scratching is presented through the Scanning Electron Microscope (SEM) images presented in Fig. 5. Figure 5(a) is an SEM image of the initial continuous Au film, while Fig. 5(b) is an SEM image (the same magnification) of the scratched film. It can be seen that the continuity of the Au film is disrupted but it is not completely removed.

The samples with the described scratch exhibit much larger  $V_m$  and  $I_m$ , as can be seen from the results presented in Fig. 4. As a matter of fact,  $V_m$  is 230 mV while  $I_m$  is 2.92 mA. Moreover, the I-V curve shape of the illuminated scratched samples now clearly resembles the S shape of the MSM photodetector devices, which is a consequence of the back-to-back Schottky diodes present in our devices.<sup>21,22</sup> The dark I-V curve of the scratched device is still dominated by the parallel resistance because of the large resistance of the diode  $S_L$ . It is also clear by the shape of the illuminated I-V curve of the scratched device in Fig. 4(b) that our devices are not appropriate for energy production, as compared to p-n or Schottky diodes. For those devices, a much larger short circuit current exists for the equivalent open circuit voltage due to the more square-like characteristics. In other words, our devices have a much smaller fill factor. They do, however, provide a small amount of harvested power, which, if we assume that the curve between  $V_m$  and  $I_m$  is linear (the equivalent of a 0.5 fill factor) and that the device area is 2 cm<sup>2</sup>, is 0.17 mW/cm<sup>2</sup>. Even at this value, though, the power produced by our device is significantly larger than the value quoted in Ref. 23 which is 4.4  $\mu$ W for a similar device of 16 cm<sup>2</sup> area. This fact reveals the importance of increasing the parallel resistance of the Au film for these types of devices. We would like to point out

that the “scratching” procedure is repeatable. We have created three different devices with the scratching method and their results are practically identical.

The measured  $V_m$  and  $I_m$  as a function of the illumination power  $E$  for the scratched device are presented in Figs. 6(a) and 6(b), respectively. Measurements from 1 sun (100 mW/cm<sup>2</sup>) down to 0.5 mW/cm<sup>2</sup> were performed. It can be easily seen that  $V_m$  is a linear function of  $E$  for the range between 50 and 0.5 mW/cm<sup>2</sup>. A linear fit, in this range, is also presented in Fig. 6(a), with the constants presented without units. The current  $I_m$  also depends linearly on  $E$ , as can be seen from Fig. 6(b) (the linear fit is presented on the figure with unitless constants). It is clear that for the presented combination of  $I_0$ ,  $R_s$ , and  $R_p$  the linear terms of Eqs. (3) and (6) dominate the behavior of this device. Then, the slope of the  $I_m$  curve can be used to determine the value of the constant  $K$  in Eq. (4). The combination of the value of  $K$  and the slope of the  $V_m$  curve can then be used to calculate the value of  $R_p$  for the scratched devices. By doing so, we calculate a value of  $n \times 136.4 \Omega$  for  $R_p$ , with  $n$  being the ideality factor of the junction. This can be compared to the value of resistance of the scratched device in the dark from Fig. 4 (we assume that the linear behavior is caused by the domination of  $R_p$ ). This value is 148.1  $\Omega$ . We believe that these values are close enough to validate the presented measurements, considering all the assumptions that have been made and the fact that the ideality factor is between 1 and 2 for most Schottky diodes. The demonstrated linearity of  $V_m$  with respect to  $E$  is the essence of the proposed photodetector. A voltage measurement is much simpler than a current measurement and our device has minimal processing (cost effective) and not only does it consume any energy but rather generates power of 7.2 nW/cm<sup>2</sup> at 0.5 mW/cm<sup>2</sup> of illumination power. It is for these three reasons we believe that the presented photodetector is very interesting for integrated, self-powered, everyday applications. Furthermore, while the concept is demonstrated for Au on Si, we believe it can be applicable for a variety of semitransparent metallic films on

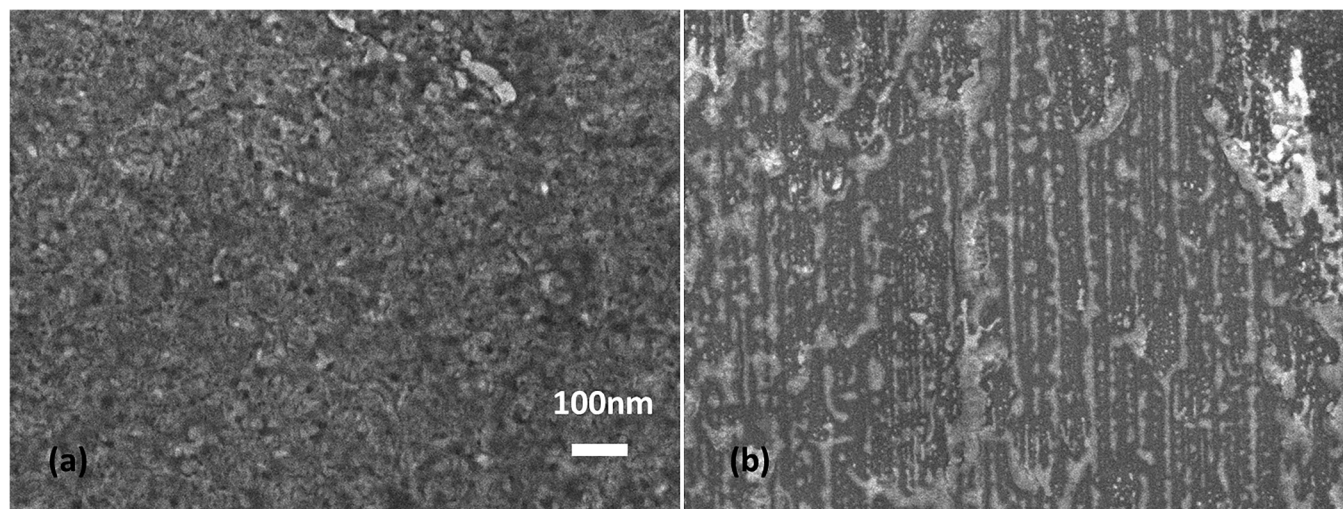
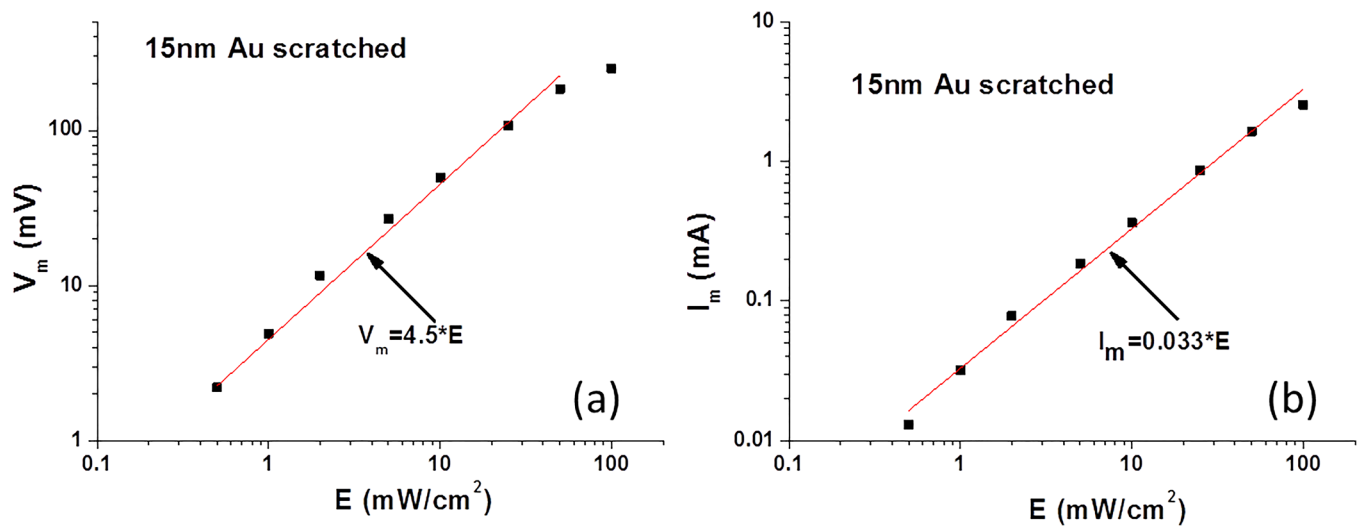


FIG. 5. SEM images of (a) the initial, continuous Au film and (b) the scratched Au film.



**FIG. 6.** (a) Open circuit voltage  $V_m$  and (b) short circuit current  $I_m$  as a function of illumination power  $E$  for the scratched devices with 15 nm of Au. The red lines represent linear fits of the data. In the presented relations, the constants are presented without units for clarity.

various insulators, provided that a Schottky contact is created and that an appropriate combination of the involved parameters exists for the linear terms to prevail.

We have to stress that the linearity of  $V_m$  with  $E$  only exists under certain combinations of  $I_0$ ,  $R_S$ , and  $R_P$  for the entire range of  $E$ . To demonstrate this, we have created devices with 7.5 nm of Au, which we have also scratched to increase their output. A simple change in the thickness of the Au film results in large changes of both  $R_S$  and  $R_P$  but also the value of the  $K$  constant.

As a result, the linear terms of Eqs. (3) and (6) do not dominate over the entire range of  $E$ . The measurement of  $V_m$  and  $I_m$ , in this case, is presented in Fig. 7. Clearly, the exponential terms of these equations dominate a much larger portion of the range of  $E$ . The linear parts only dominate in the lower  $E$  range, where the values of  $V_m$  and  $I_m$  are smaller, as expected. The linear and logarithmic fits of each range are presented in the figure along with the corresponding equations (as before the constants are presented without units).

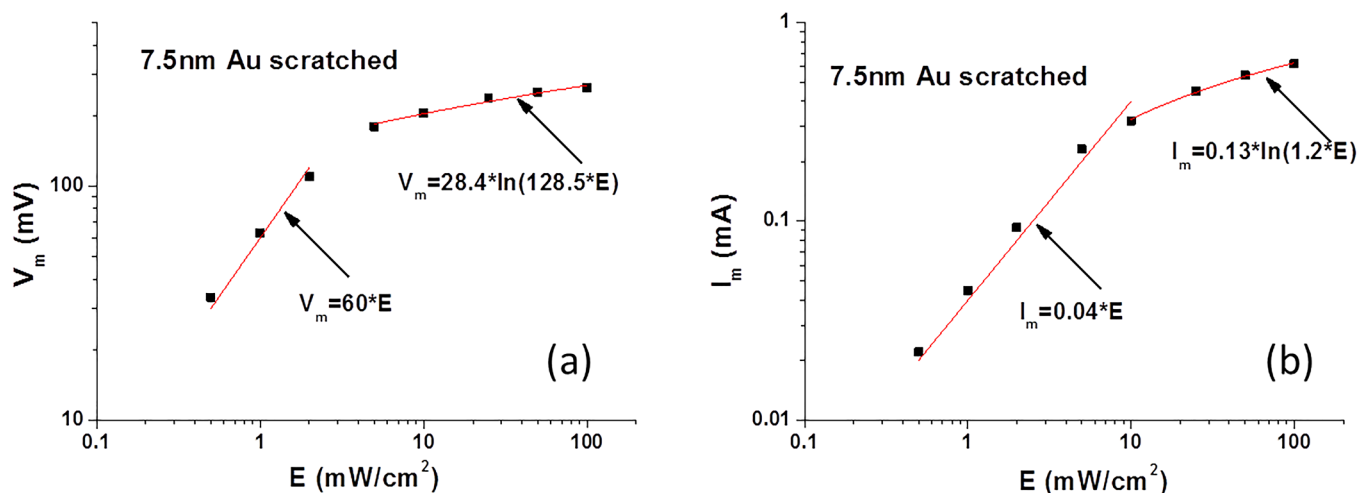


**FIG. 7.** (a) Open circuit voltage  $V_m$  and (b) short circuit current  $I_m$  as a function of illumination power  $E$  for the scratched devices with 7.5 nm of Au. The red lines represent linear fits of the data. In the presented relations, the constants are presented without units for clarity.

From the results presented in Fig. 6, it becomes clear that the presented photodetector's main advantages are its linear output voltage with respect to illumination power, its ability to self-power through energy harvesting, and its cost effective fabrication process. The latter can be compared favorably against all other existing photodetectors that need at the very least implantation and high temperature annealing to create the appropriate ohmic contacts, in addition to metallization and lithography steps. In terms of building a sensor system, a large part of the cost is associated with the creation of the accompanying energy source and readout electronics, as well. The self-powering of our device would reduce the energy needs of such a system. Moreover, the offered possibility of measuring voltage, instead of current, not only simplifies the readout circuitry but also reduces the energy consumption of such a system. So, even though typical photodetectors, such as the pn junction ones, offer larger accuracies due to the larger current response to changes in illumination power, our photodetector offers an attractive alternative for cost and not performance driven applications.

## CONCLUSIONS

In conclusion, we demonstrate a novel, integrable, self-powered, and cost effective photodetector. The photodetector consists of a semitransparent, 15 nm thick, Au layer deposited on a n-type Si substrate scratched in the middle by tweezers. We use the "shadow effect," namely, masking half of the device under illumination to create anisotropy. With this extremely simple device structure, we show that under certain conditions of built-in series and parallel resistance the open circuit voltage is a linear function of the illumination power and is therefore appropriate for detecting the intensity of light. Moreover, we show that these devices can produce small amounts of power even at an illumination power of  $0.5 \text{ mW/cm}^2$  and can therefore be considered self-powered. We show that the reason for this behavior is the fact that this device consists of back-to-back Schottky diodes with a rather small parallel resistance across them. We believe that the demonstrated photodetector can be very useful in everyday applications such as car and house smart lighting, smart shading, and others where cost outweighs performance.

## ACKNOWLEDGMENTS

This work has received funding from the Hellenic Foundation for Research and Innovation (HFRI) and the General Secretariat for Research and Technology (GSRT), under Grant Agreement No. 27361/21-02-2019.

## DATA AVAILABILITY

The data that support the findings of this study are available within the article.

## REFERENCES

- W. Tian, Y. Wang, L. Chen, and L. Li, *Small* **13**, 1701848 (2017).
- N. Horiuchi, *Nat. Photonics* **12**, 644 (2018).
- Z. L. Wang, J. Chen, and L. Lin, *Energy Environ. Sci.* **8**, 2250 (2015).
- B. Dong, Q. Shi, Y. Yang, F. Wen, Z. Zhang, and C. Lee, *Nano Energy* **79**, 105414 (2021).
- Z. Li, Q. Zheng, Z. L. Wang, and Z. Li, *Research* **2020**, 1 (2020).
- S. M. Sze, *Physics of Semiconductor Devices*, 3rd ed. (Wiley, Hoboken, NJ, 2007).
- A. O. Goushcha, B. Tabbert, Y. Petraitis, A. Harter, E. Bartley, and L. Walling, *J. Appl. Phys.* **123**, 044505 (2018).
- R. L. Petritz, *Phys. Rev.* **104**, 1508 (1956).
- J. Liu, Y. Liang, L. Wang, B. Wang, T. Zhang, and F. Yi, *Mater. Sci. Semicond. Process.* **56**, 217 (2016).
- K. Yoo, S. Biswas, Y. J. Lee, S. C. Shin, K. J. Kim, J. W. Shim, H. Kim, and J. J. Lee, *IEEE Access* **8**, 114752 (2020).
- C. A. Reynaud, R. Clerc, P. B. Lechêne, M. Hébert, A. Cazier, and A. C. Arias, *Sol. Energy Mater. Sol. Cells* **200**, 110010 (2019).
- W. Tress, M. Yavari, K. Domanski, P. Yadav, B. Niesen, J. P. Correa Baena, A. Hagfeldt, and M. Graetzel, *Energy Environ. Sci.* **11**, 151 (2018).
- J. J. Lof, *Light Intensity Dependence of the Open-Circuit Voltage in Organic Bulk Heterojunction Solar Cells* (University of Groningen, 2014).
- I. Raifuku, Y. Ishikawa, S. Ito, and Y. Uraoka, *J. Phys. Chem. C* **120**, 18986 (2016).
- M. Chegaar, A. Hamzaoui, A. Namoda, P. Petit, M. Aillerie, and A. Herguth, *Energy Procedia* **36**, 722 (2013).
- S. Qiao, R. Cong, J. Liu, B. Liang, G. Fu, W. Yu, K. Ren, S. Wang, and C. Pan, *J. Mater. Chem. C* **6**, 3233 (2018).
- S. Qiao, J. Liu, X. Niu, B. Liang, G. Fu, Z. Li, S. Wang, K. Ren, and C. Pan, *Adv. Funct. Mater.* **28**, 1707311 (2018).
- J. Duran and A. Sarangan, *IEEE Photonics J.* **11**, 6800215 (2019).
- A. Di Bartolomeo, *Phys. Rep.* **606**, 1 (2016).
- M. Farhat, S. Kais, and F. H. Alharbi, *Sci. Rep.* **7**, 1 (2017).
- A. Behnam, J. Johnson, Y. Choi, L. Noriega, M. G. Ertosun, Z. Wu, A. G. Rinzler, P. Kapur, K. C. Saraswat, and A. Ural, *J. Appl. Phys.* **103**, 114315 (2008).
- A. Aissat, M. El Besseghi, and D. Decoster, *International Conference on Multimedia Computing and Systems Proceedings* (IEEE, 2014), p. 1392.
- Q. Zhang, Q. Liang, D. K. Nandakumar, S. K. Ravi, H. Qu, L. Suresh, X. Zhang, Y. Zhang, L. Yang, A. T. S. Wee, and S. C. Tan, *Energy Environ. Sci.* **13**, 2404 (2020).
- S. K. Ravi, W. Sun, D. K. Nandakumar, Y. Zhang, and S. C. Tan, *Sci. Adv.* **4**, eaao6050 (2018).
- S. K. Ravi, Y. Zhang, Y. Wang, D. K. Nandakumar, W. Sun, M. R. Jones, and S. C. Tan, *Adv. Energy Mater.* **9**, 1901449 (2019).
- Q. Zhang, Q. Liang, D. K. Nandakumar, H. Qu, Q. Shi, F. I. Alzakia, D. J. J. Tay, L. Yang, X. Zhang, L. Suresh, C. Lee, A. T. S. Wee, and S. C. Tan, *Nat. Commun.* **12**, 1 (2021).
- R. W. Soshea and M. M. Atalla, *IRE Trans. Electron Devices* **9**, 510 (1962).
- R. Balsano, A. Matsubayashi, and V. P. Labella, *AIP Adv.* **3**, 112110 (2013).
- A. Axelevitch, B. Gorenstein, and G. Golan, *Phys. Procedia* **32**, 1 (2012).
- S. Qiao, B. Liang, J. Liu, G. Fu, and S. Wang, *J. Phys. D: Appl. Phys.* **54**, 153003 (2021).
- G. Lucovsky, *J. Appl. Phys.* **31**, 1088 (1960).
- J. Wallmark, *Proc. IRE* **45**, 474 (1957).
- T. Dittrich, *Materials Concepts for Solar Cells*, 2nd ed. (World Scientific, London, 2018), pp. 3–43.